**Full article title: Sex-specific transcriptomic profiling of reward and sensory brain areas in perinatal fentanyl exposed juvenile mice.**

Jimmy Olusakin[1,2], Gautam Kumar[1,2], Mahashweta Basu[3], Cali A. Calarco[1,2], Megan E. Fox[4], Jason B. Alipio[1,2], Catherine Haga[1,2], Makeda D. Turner[1], Asaf Keller[1,2,5], Seth A. Ament[2,3,5], Mary Kay Lobo[1,2,5]

[1]Department of Anatomy and Neurobiology, University of Maryland school of Medicine, Baltimore, Maryland.
[2]Program in Neuroscience, University of Maryland School of Medicine, Baltimore, Maryland.
[3]Institute for Genome Sciences, University of Maryland School of Medicine, Baltimore, Maryland.
[4]Department of Anesthesiology, Penn State college of Medicine, Hershey, Pennsylvania.
[5]Department of Psychiatry, University of Maryland School of Medicine, Baltimore, Maryland.

Corresponding author: Dr Mary Kay Lobo, Professor of Neurobiology, University of Maryland, School of Medicine. mklobo@som.umaryland.edu

**Short title: Brain transcriptomes in perinatal fentanyl mice.**

Keywords: fentanyl, perinatal, transcript, sex differences, reward, sensory.

## ABSTRACT

BACKGROUND: Use of the synthetic opioid fentanyl increased ~300% in the last decade, including among women of reproductive ages. Adverse neonatal outcomes and long-term behavioral disruptions are associated with perinatal opioid exposure. Our previous work demonstrated that perinatal fentanyl exposed (PFE) mice displayed enhanced negative affect and somatosensory circuit and behavioral disruptions during adolescence. However, little is known about molecular adaptations across brain regions that underlie these outcomes. We performed RNA-sequencing across three reward and two sensory brain areas to study transcriptional programs in PFE juvenile mice.

METHODS: C57BL/6 pregnant dams received 10μg/ml fentanyl in the drinking water from embryonic day 0 (E0) through gestational periods until weaning at postnatal day 21 (P21). RNA was extracted from nucleus accumbens (NAc), prelimbic cortex (PrL), ventral tegmental area (VTA), somatosensory cortex (S1) and ventrobasal thalamus (VBT) from PFE mice of both sexes at P35. RNA-sequencing was performed, followed by analysis of differentially expressed genes (DEGs) and gene co-expression networks.

RESULTS: Transcriptome analysis revealed sex-specific DEGs and gene modules significantly associated with PFE. The VTA had the most DEGs, while pronounced gene enrichment occurred in NAc. Genes enriched in mitochondrial respiration were pronounced in NAc and VTA of PFE males, extracellular matrix (ECM) and neuronal migration enrichment were pronounced in NAc and VTA of PFE males, while genes associated with vesicular cycling and synaptic signaling were markedly altered in NAc of PFE female mice. In sensory areas from PFE females, we found alterations in mitochondrial respiration, synaptic and ciliary organization processes.

CONCLUSION: Our findings demonstrate sex-specific neuroadaptations in PFE mice. Our studies identify distinct transcriptomes across reward and sensory brain regions that may underlie disrupted behavioral and circuit states in PFE mice.

## INTRODUCTION

The opioid epidemic is one of the most severe and intractable public health crises in US history (1). Fentanyl and other potent synthetic opioid analogs, which are 50-100 times more potent than morphine, are commonly added to illicit drugs, increasing fentanyl exposure and driving opioid-related overdose deaths (1). In 2016, about 11.5 million people reported opioid misuse, out of which 18.2% met criteria for an opioid use disorder (OUD) (*https://www.samhsa.gov/data/*). Women of reproductive age are among individuals with OUD, and between 14% and 29% of pregnant women filled at least one opioid prescription during pregnancy (2). Opioid use during pregnancy predisposes babies to withdrawal symptoms, premature births, decreased birth weight and body size, and, in extreme cases, stillbirth and infant death (3), (4). There is also the risk of opioid dependent babies born with neonatal abstinence syndrome (NAS). Long term consequences of prenatal and perinatal opioid exposure include dysregulated stress reactivity, altered glucocorticoid levels, hyperactivity, impulsivity and aggression (5). Perinatal opioid exposure can also produce delayed sensory milestones in preclinical models and human offspring (6), (7), as well as abnormal pain sensitivity (8). Opioids cross the placental barrier, entering fetal circulation and the central nervous system where they may affect fetal brain development. Understanding the neuro-molecular signatures and transcriptional substrates resulting from developmental opioid exposure that may mediate long term behavioral phenotypes has been challenging. Preclinical studies describing the molecular and cellular changes in endogenous opioid and neurotransmitter signaling often focus on isolated brain regions canonically associated with addiction and the reward-related behaviors and sensory areas (9), (10), (11). Sex as a variable need also be considered in understanding the consequences of perinatal opioid exposure (12).

We recently developed a perinatal fentanyl exposure (PFE) model to mimic and capture the human embryonic developmental exposure period (11), (13). PFE mice show signs of withdrawal, decreased exploratory and reduced motivated behavior (11), (13) suggesting a direct action of fentanyl during early development. In the current study, we investigated sex-specific transcriptional programs occurring at adolescent ages in PFE mice in reward-related and sensory brain areas that are implicated in long lasting behavioral sequalae observed in PFE.

## METHODS AND MATERIALS

Experimental subjects

All experiments were performed in accordance with the Institutional Animal Care and Use Committee guidelines at the University of Maryland School of Medicine (UMSOM). C57BL/6 control mice were given food and water *ad libitum* and housed in UMSOM animal facilities on a 12:12 h light:dark cycle.

Fentanyl administration

Upon determination of pregnancy, C57BL/6 mice were singly housed. Each dam was provided with a single 50 mL falcon tube with a rubber stopper and ball-point sipper tube (Ancare) containing 10µg/mL fentanyl citrate (Cayman #22659) in water as their sole liquid source for embryonic day 0 (E0) through gestation till weaning of pups at postnatal day 21 (P21). Control mice received plain water in identical 50 mL tubes. Fentanyl or water consumption was determined by weighing the tubes daily and normalized to individual mouse body weight. After weaning pups at P21, pups were grouped housed with same-sex littermates and given food and water *ad libitum* until P35.

Tissue collection and RNA extraction

At P35, tissue punches were collected from 4 juvenile mice/group/sex as follows, prelimbic cortex (PrL) with a single midline 12-gauge, ventral tegmental area (VTA) with a single midline 14-gauge, nucleus accumbens (NAc) and ventrobasal thalamic nuclei (VBT) with bilateral 14-gauge and primary somatosensory cortex (S1) with bilateral 15-gauge and stored at -80 ºC until ready for RNA processing. RNA extraction was performed as previously described (14). Briefly, RNA was extracted using Trizol (Invitrogen) and the RNeasy Mini kit (#74104, Qiagen) with a DNase step (#79254, Qiagen). RNA quantity and integrity was measured using a Nanodrop (ThermoScientific).

RNA sequencing and RNAseq data analysis

For RNA sequencing, only samples with RNA integrity numbers >8 were used. Samples were submitted in biological quadruplicates for RNA sequencing at the UMSOM Institute for Genome Sciences (IGS) and processed as described previously (15). Libraries were prepared from 10 ng of RNA from each sample using the SMART-Seq

v4 kit (Takara). Samples were sequenced on an Illumina HiSeq 4000 with a 75 bp paired-end read. 64–100 million reads were obtained for each sample. Reads were aligned to the mouse genome (*Mus musculus*. GRCm38) using TopHat2 (version 2.0.8; maximum number of mismatches = 2; segment length = 30; maximum multi-hits per read = 25; maximum intron length = 50,000). The number of reads that aligned to the predicted coding regions was determined using HTSeq. We applied two strategies to characterize gene expression changes in these data. First, we identified individual genes with significant gene expression changes following perinatal fentanyl exposure. We used limma-trend to fit log2-normalized read counts per million to a linear model and tested for significant effects of fentanyl in each brain area, separately in males and in females, as well as treating sex as a covariate (*See Supplementary data 1 for methodology of gene analysis*). In our primary analysis, we set a False Discovery Rate (FDR) < 0.05 to define differentially expressed genes. We used a threshold-free approach, Rank-Rank Hypergeometric Overlap (RRHO), to compare effects between connected brain areas. For functional enrichment analysis, we analyzed sets of fentanyl-associated genes with FDR < 0.05 and fold change (FC) +/- 0.3. We also considered a broader set of fentanyl-associated genes with (uncorrected) p-values < 0.05. Analysis of over-represented Gene Ontology (GO) terms were performed with clusterProfiler 4.0 and gprofiler2 for R, and Metascape (using default enrichment parameters, *http://www.metascape.org*) (16) for functional enrichment analysis. iRegulon plugin on Cytoscape 3.0 (17) was used to predict transcription factors, targets and binding motifs. In addition, we characterized the effects of fentanyl on gene co-expression networks. As a starting point for this analysis, we used limma-trend to select the set of genes that exhibited a nominally-significant effect (p-value < 0.05) of fentanyl or sex. We then used weighted gene co-expression network analysis (WGCNA) to characterize co-expressed modules among these genes, separately across all 5 brain areas (*See Supplementary data 4 for methodology of WGCNA analysis*). Module detection was performed with the blockwiseModules() function with power = 10, corType = 'bicor', networkType = 'signed', minModuleSize = 25, reassignThreshold = 0, mergeCutHeight = 0.25, minMEtoStay = 0, and otherwise default parameters. We tested for differential expression of module eigengenes with limma, using posthoc contrasts to estimate effects of fentanyl while adjusting for sex differences, as above. Hub genes for each module were defined by calculating the Pearson correlation between the eigengene and each gene in the module. For functional enrichment analyses of network modules, we used gprofiler2,

in which genes were ranked by their module membership scores, with hub genes ranked highest. We report the most re-occurring enriched terms to describe each module.

## RESULTS

### Perinatal fentanyl exposure induces sex-specific gene expression changes in reward and sensory brain regions of juvenile mice.

Pregnant C57BL/6 dams received 10μg/ml fentanyl in their drinking water from embryonic day 0 (E0) through birth until weaning at postnatal day 21 (P21). Post-weaning, at P35, we performed an unbiased transcriptomic analysis in PFE mice using high-throughput RNAseq of bulk-tissue punches from VTA, NAc, PrL, S1 and VBT from four juvenile (P35) mice per sex/treatment (Fig. 1A). We used two parallel streams of analyses – first identifying sex-specific differentially expressed genes (DEGs) in each brain region and testing for functional enrichments as well as evaluating the overlap of differential expression between pairs of interconnected brain regions with a Rank rank hypergeometric overlap analysis and second, using a weighted gene correlation network analysis (WGCNA) approach allowing us to cluster genes dysregulated by perinatal fentanyl exposure into modules.

A total of 2,920 genes were differentially expressed between the PFE and control groups in male and/or female mice in at least one of the five tissues (henceforth, "PFE DEGs"; FDR < 0.05; *Supplementary data 2).* We identified more DEGs in the VTA (2,935 DEGs) and NAc (889 DEGs) compared to S1 (311 DEGs), VBT (131 DEGs), or PrL (5 DEGs) (Fig. 1B). Notably, the vast majority of these DEGs were sex-specific, with just 28, 3, and 2 DEGs detected at FDR < 0.05 in common between both sexes in VTA, NAc, and VBT, respectively, and none in S1 and PrL (Fig. 1B,C). To confirm the sex-specificity of these effects, we also considered a broader set of genes with trend effects (uncorrected p-values < 0.05 in each sex/tissue), identifying similar patterns (Fig. S1A). Heatmaps of the PFE DEGs common to males and females at both FDR < 0.05 (Fig. 1E,F) and $P < 0.05$ (Fig. S1A) showed that PFE generally had similar effects in males and females in PrL, VTA and S1. However, in NAc and VBT, many of these "common" PFE DEGs were actually affected in opposite directions in males vs. females (Fig. S1A). In summary, perinatal fentanyl exposure had dramatic effects on gene expression in VTA and NAc, most of which were sex-specific.

We performed functional enrichment analyses of both common and sex-specific effects PFE DEGs to gain insight into the biological consequences of perinatal fentanyl. Functional enrichment analyses of common and sex-specific DEGs suggested that the strongest effects of PFE are on the expression of genes related to mitochondrial respirasome and structural ribosomal constituents (Fig. 1D-F; Fig. S1B; *Supplementary Data 3*). In particular, genes related to complex 1 NADH:ubiquinone oxidoreductase (*Nduf*) were differentially expressed in a sex-dependent manner across most of the brain regions assessed, with the strongest effects in the NAc and VTA of males and S1 of female mice. Interestingly, these *Nduf* genes were upregulated in male NAc and female S1 but were downregulated in the VTA of both sexes (Table 1). This could indicate an increase in active protein synthesis and cellular energy production in S1 and NAc of females and males respectively while a decrease in cellular energy production in the VTA.

PFE was also associated with gene expression changes in pathways with functions more specific to neurons. We observed downregulation of collagen type (*Col*) genes specifically in males in both NAc and VTA (Fig. 1D, Table 2). These collagens are components of the extracellular matrix (ECM) and play a critical role in regulation of myriad cellular and structural functions ranging from cell migration, angiogenesis to inflammation (18), (19). In NAc, PFE was also associated with down-regulation of synaptic and vesicular signaling genes, primarily in females (Table 3). Downregulation of these genes could suggest aberrant neurogenesis in the mesolimbic pathways particularly the NAc in female PFE mice.

**Effects of perinatal fentanyl on ECM, mitochondrial respiration and synaptic processes are correlated across brain reward and sensory brain regions.**

Next, we sought to compare the effects of PFE across brain regions. For this purpose, we performed a two-sided rank-rank hypergeometric overlap analysis (RRHO) to identify patterns and strength of genome-wide overlap in a threshold-free manner. RRHO analyses between PrL-NAc strengthened the directional regulation of genes enriched in structural constituent of ribosome and mitochondrial respiration as this enrichment occurred in upregulated genes between PrL-NAc (Fig. 2A). Complementary to our finding of ECM/neuronal guidance enrichment in downregulated male NAc genes, RRHO analysis between PrL-NAc showed a downregulation of

genes enriched in growth factor binding and ECM. Lastly, NAc-VTA RRHO enrichment analysis showed a downregulation of genes enriched in post-synapse and intracellular signal transduction. This enrichment aligns with the synaptic and MAP kinase activity observed in downregulated genes in female NAc (Fig. 1D and Supplementary 2) suggesting that synaptic remodeling occurs in the female NAc following PFE.

Furthermore, RRHO between the VBT-S1 revealed that regulation of neuron projection development, *SH2* domain binding, blood vessel morphogenesis and adherens junction were enriched in downregulated genes (Fig. 2C). SH2 domains are integral to receptor tyrosine kinase signaling (21) and SH2 is an integral regulator of endothelial specific cadherins that localizes to adherens junctions (22), (23) . This suggests that endothelial vessels may be perturbed during development in fentanyl exposed mice.

**Network analyses reveals sex-specific transcriptional signatures correlated with PFE.**

To better resolve gene networks associated with fentanyl exposure, we performed Weighted Gene Co-expression Network Analysis (WGCNA) for each brain region separately, identifying 10 to 46 gene co-expression modules per brain region (reward areas: Fig. 3A,B; sensory areas: Fig. 4A,B). We used linear models to test the sex-specific associations of each module with fentanyl treatment. We identified 7 fentanyl-associated modules in the NAc, 8 in the PrL and 6 in the VTA (Fig. 3C and D). S1 and VBT each had 7 fentanyl-associated modules (Fig. 4C and D). Gene set enrichment analyses identified functional categories enriched in many of these modules (Fig. 3E and Fig. 4E). In the NAc and VTA, 11 out of the 13 significant modules contained genes positively associated with PFE only in males (Fig. 3D). All PrL significant modules showed positive association with fentanyl when sexes were combined. Five of 8 modules had downregulated genes – one module each, “turquoise” and “green” were specifically driven by gene expression changes in females and in males, respectively (Fig. 3D). Three modules in the PrL contained upregulated genes, with one association driven specifically by gene expression changes in females.

In reward brain regions, we identified histone methylation, angiogenesis, mitochondria (Fig. 3E) – processes described to be dysregulated in adult opioid use disorder (24)–(26) suggesting that PFE abnormalities persists into adulthood. Interestingly, we find in the NAc “hot pink” module the highest enrichment for mitochondrial respiration

and structural ribosomal terms specifically in upregulated male genes. Angiogenesis was enriched in downregulated male genes in NAc "light green" module, in line with our observation from NAc RRHO enrichment analyses (Fig. 2B, 3B and C). In the PrL, although no obvious enrichment was seen with regional analyses, modular analyses revealed significant enrichment in ciliary assembly and neuronal projection morphogenesis. In the VTA, the only module associated with PFE female upregulated genes was enriched in mesenchymal cell differentiation (Fig. 3E). The remaining 5 modules were enriched in metabolic processes.

In the S1 cortex there was a greater association of fentanyl with genes differentially expressed in females. Specifically, 4 of 7 modules contained female genes – 2 contained upregulated and 2 contained downregulated genes (Fig 4D). The VBT, however, had equal number of sex specific modules associated with fentanyl. Structural ribosomal constituent was enriched in upregulated female modular "brown module" further strengthening our observation with regional DEGs enrichment (Fig. 1E). Terms of interest that were revealed by the enrichment analyses in S1 were myelination, monoamine/serotonin transport and Golgi organization. These processes have been shown to be dysregulated in substance use disorder (27), (28). Our study highlights sex preferences for these processes. Specifically, serotonin transport was enriched in upregulated male genes; Golgi organization was downregulated female genes. Myelination did not display a sex specific enrichment, but it was enriched in upregulated modules occurring in both sexes.

Since our GO term analysis suggested common recurrent functional enrichment processes altered by PFE, we then sought to find potential transcriptional regulators for these processes (Fig. 5). We used the transcriptional regulator analysis iRegulon on genes from significant GO terms. We show the top 5 predicted transcriptional regulators based off their normalized enrichment score (NES). We identified 3 zinc finger transcription factors predicted to regulate genes associated with metabolic processes and RNA processing across the reward areas (Fig. 5). Specifically, *Zfp143* (zinc finger protein 143), a transcriptional activator, is predicted to regulate target genes involved in intracellular transport, mitochondrial respiration, ATP metabolic processes across all three reward areas. *Yy2* (yin yang 2 or zinc finger protein 631), a transcription factor which possess both activation and repression domains regulates genes involved in RNA processing across all reward areas. *Zbtb33* (zinc finger And BTB domain

containing 33) regulated genes enriched in peptide biogenesis, mitochondrial respiration, histone modification and RNA processing/protein localization across the NAc and PrL.

In two PrL modules enriched in ciliary assembly and morphogenesis, we identified *Tfap2a* (Transcription factor AP2 alpha) and *Mef2c* (Myocyte enhancer factor 2C) transcription factors involved in regulation of neuronal development and distribution and early morphogenesis. *Six6* (Sine oculis homeobox homolog 6) and *Gcm1* (Glial cells missing transcription factor 1) are two ciliary assembly transcription factors with known roles in development (29, 30)

## DISCUSSION

We present a comprehensive profile of transcriptional programs dysregulated in a sex-specific manner in juvenile mice exposed perinatally to fentanyl. The novelty in our study describes sex-specific differentially expressed transcriptional programs and altered biological processes in three reward areas – NAc, PrL and VTA and two sensory areas - S1 and VBT. The PFE paradigm we used is based on an established model (11), (13) that displays negative affective behaviors, such as heightened anxiety-like behaviors and sensory deficits, including defective sensory adaptation (11) and reduced pain sensitivity (8) behaviors at juvenile ages. We used two parallel analysis streams and show convergence between these analyses. Our primary DEG analyses showed that the VTA had the greatest number of common and sex-specific DEGs between males and females regulated by PFE. The VTA has a fundamental role in opioid dependence and withdrawal, including neuronal structural and functional plasticity particularly elicited by opioid use and exposure, which could explain the high transcriptional substrates we observed in our PFE data. The prefrontal cortex including its PrL region undergoes a protracted development and substantial remodeling throughout adolescence (31). Previous studies have observed attenuated neuronal activity in the PrL of adolescent rats following heroin self-administration (32). In this study, we did not observe substantial DEGs regulating PFE in the PrL of both sexes probably due to a number of factors – (1) due to the protracted development and dynamic changes occurring in this brain area, there might not be quantifiable significant effect of PFE, (2) variability in gene expression among biological samples. On the other hand, WGCNA which takes advantage of some of the pitfalls of DEG analysis to highlight higher-order relationships among genes revealed significant modules associated with PFE. *Gdpd4* – Glycerophosphodiester phosphodiesterase domain containing 4 to be downregulated in PrL of PFE male mice. *Gdpd4* is one of five family of *Gdpd* and strongly expressed in testes of male mice. It has been reported that no overt developmental or fertility abnormalities in Gdpd4 mutant mice (33), however, inherited or de novo copy number variants encompassing Gdpd4 were found in human patients with autism (34). In PFE females, downregulation of Bone morphogenetic protein 1 (*Bmp1*) could indicate abnormal maturation of diverse ECM proteins as well as precocious activation of TGF-ß related growth factors (35).

NAc DEG enrichment analyses reveal mitochondria respiration, structural ribosomal processes and RNA processing were upregulated in the male PFE condition. Our RRHO analysis of PrL-NAc and NAc-VTA also show

upregulation of genes enriched in mitochondrial respiration, structural ribosome and RNA processing, indicative of increased energy demands in the NAc. Mitochondrial dynamics is key to drug seeking and abstinence. Our lab previously showed increase in mitochondria fission related to excitatory synaptic function in NAc D1-MSNs and drug seeking behavior of mice that administered cocaine (36). We found the mitochondria complex 1 genes (*Ndufs*) were altered by PFE. These genes were particularly upregulated in the male NAc and female S1 suggesting increase energy demands in these brain areas. However, most observed *Nduf* genes in the VTA were downregulated in both sexes. While we cannot directly determine if these changes in mitochondrial respiratory genes in our PFE reflects mitochondrial dysfunction or a higher metabolic demand, we observed dual specificity phosphatase 14 (*Dusp14)*, an immediate early gene (IEG) that is regulated in response to oxidative damage, to be upregulated in NAc of PFE males. In line with this, Wojcieszak and colleagues found *Dusp14* among IEGs upregulated in mice striatum in response to acute synthetic cathinone administration (37). In addition, we found the cytosolic antioxidant, Glutathione S-transferase mu 5 (*Gstm5*), to be upregulated in NAc of males, which could reflect a possible response to the increase in oxidative stress. Similar changes in these mitochondrial oxidative stress genes were observed in the striatum of mouse model of Parkinson's disease (38).

Our study shows that male PFE mice displayed alterations in ECM molecules. The ECM provides proper structural stability in synaptic function, blood-brain barrier integrity and cell-to-cell communication (19), (39). ECM macromolecules are essential for crafting the cellular domains required during development and morphogenesis (18). Male PFE mice had the greatest perturbations in ECM and neuronal guidance molecules. Proper ECM development and signaling is necessary in setting up brain architecture, opioids impact ECM and sexual dimorphism in ECM has been observed across species (19), thus consideration of ECM in brain development during opioid exposure of both sexes is paramount. Indeed, we observed downregulation of Collagen type molecules (*Col*) and the *Notch* intracellular signaling molecules specifically in the NAc and VTA of male PFE mice. Our modular enrichment analyses demonstrate highest enrichment of ECM in NAc modules significantly associated with PFE males. This was in line with NAc DEG analysis showing ECM enrichment in downregulated male genes. In agreement with our finding, there is a wealth of studies showing that opioids can modulate different classes of ECM signaling molecules in a cell type specific manner (19), (30-43). Additionally, we find the ECM secreted

guidance molecules – *Slits* and *Plexins* specifically downregulated in male NAc and VTA. This is in line with previous studies showing that morphine or oxycodone self-administration altered axonal guidance and micro-RNAs in the ventral striatum in mice (44, 45).

While the NAc enrichment analyses showed that ECM was altered in PFE males, synaptic signaling dysregulation was more pronounced in PFE females. Dendritic atrophy and spine loss of medium spiny neurons (MSNs) in the NAc of adult rats following opioid administration has been reported across multiple studies (46)–(48). Recently, our group showed that fentanyl abstinence in adult mice decreases dendritic complexity in D1-MSNs of the NAc (49) and this has been shown to be associated with negative affective states (50-52). Interestingly, we found genes essential for dendritic development altered in this PFE study. Specifically, Neurogenic differentiation factor 1 (*NeuroD1*), a transcriptional activator that is required for dendritic morphogenesis and Netrin G2 (*Ntng2*), that promotes neurite outgrowth of both axons and dendrites downregulated in NAc of females. This decrease in dendritic complexity particularly in NAc of female PFE mice could further reinforce the 'telescoping' effect of a rapid progression from initiation of opioid use to an opioid use disorder observed in females (53). Brain immune responses, including phagocytic microglia, can sculpt neuronal architecture (54). Previous studies have shown that perinatal methadone administration increases inflammatory cytokines and chemokines in the neonatal brain while priming the peripheral immune system (55). Interestingly we observed enrichment of immune responses particularly in VTA of female PFE in trending upregulated genes (uncorrected $p < 0.05$).

Our iRegulon analysis was an in silico approach to predict transcriptional factors regulating functional categories over-represented within module genes. We find in the reward brain areas, iRegulon predicted transcription factors seem to play vast regulatory roles during brain development (56, 57) and gene regulatory roles for functional categories within our analysis. Specifically, we found *Zfp143* (Staf, selenorysteine RNA gene transcription activating factor) consistently enriched for mitochondrial and intracellular transport across brain regions. Although *Zfp143* expression was present in our data across all brain regions, it did not meet our DEG filtering criteria. Investigations on Zfp143 has mainly focused on its transcriptional changes following ethanol consumption (58), (59). An understanding of how changes in its expression level and activity modulates developmental opioid consumption warrants further investigation.

In conclusion, our findings elucidate that PFE induces sex-specific transcriptional alterations in reward and sensory brain areas with marked changes in the NAc, VTA and S1 areas. PFE male juvenile mice showed the most transcriptional perturbations specifically in processes relating to mitochondrial respiration, ECM and neuronal guidance. PFE female mice showed transcriptional alterations in genes enriched for vesicular and synaptic signaling processes. The altered functional enrichment we observe are consistent with opioid induced gene enrichment described in the literature. We highlight that these altered processes have a developmental root and as such early intervention beginning precisely at the early stages of abstinence may prevent or reduce some of these neuro-molecular changes and possibly behavioral adaptations.

**Acknowledgements**

This work was supported by NIH R01DA038613 (to MKL, SAA, and AK), R01DA054905 (to MKL), University of Maryland Strategic Partnership Empowering the State, and University of Maryland School of Medicine (UMSOM) Center for Substance Use in Pregnancy. The authors also thank the UMSOM Institute for Genome Sciences for RNA-seq services.

**Disclosures**

The authors have no biomedical financial interests or potential conflicts of interest to report.

REFERENCES


1. Volkow ND, Blanco C (2021): The changing opioid crisis: development, challenges and opportunities. *Molecular psychiatry*, *26*(1), pp.218-233.
2. Grecco GG, Atwood BK (2020): Prenatal Opioid Exposure Enhances Responsiveness to Future Drug Reward and Alters Sensitivity to Pain: A Review of Preclinical Models and Contributing Mechanisms. *Eneuro*, *7*(6).
3. Jansson LM, Velez M, Harrow C (2009): The opioid exposed newborn: assessment and pharmacologic management. *Journal of opioid management*, *5*(1), p.47.
4. Reddy UM, Davis JM, Ren Z, Greene MF (2017): Opioid use in pregnancy, neonatal abstinence syndrome, and childhood outcomes: executive summary of a joint workshop by the Eunice Kennedy Shriver National Institute of Child Health and Human Development, American Congress of Obstetricians and Gynecologists, American Academy of Pediatrics, Society for Maternal-Fetal Medicine, Centers for Disease Control and Prevention, and the March of Dimes Foundation. *Obstetrics and gynecology*, *130*(1), p.10.
5. Ornoy A, Michailevskaya V, Lukashov I, Bar-Hamburger R, Harel S (1996): The developmental outcome of children born to heroin-dependent mothers, raised at home or adopted. *Child abuse & neglect*, *20*(5), pp.385-396.
6. Hudak ML, Tan RC, Committee on Drugs, Committee on Fetus and Newborn, Frattarelli DA, Galinkin JL, Green TP, Neville KA, Paul IM, Van Den Anker JN, Papile LA (2012): Neonatal drug withdrawal. *Pediatrics*, *129*(2), pp.e540-e560.
7. Grecco GG, Huang JY, Muñoz B, Doud EH, Hines CD, Gao Y, *et al*. (2022): Sex-Dependent Synaptic Remodeling of the Somatosensory Cortex in Mice With Prenatal Methadone Exposure. *Advances in Drug and Alcohol Research*, p.5.
8. Wallin CM, Bowen SE, Roberge CL, Richardson LM, Brummelte S (2019): Gestational buprenorphine exposure: effects on pregnancy, development, neonatal opioid withdrawal syndrome, and behavior in a translational rodent model. *Drug and Alcohol Dependence*, *205*, p.107625.
9. Bruijnzeel AW, Gold MS (2005): The role of corticotropin-releasing factor-like peptides in cannabis, nicotine, and alcohol dependence. *Brain research reviews*, *49*(3), pp.505-528.
10. Liu J, Pan H, Gold MS, Derendorf H, Bruijnzeel AW (2008): Effects of fentanyl dose and exposure duration on the affective and somatic signs of fentanyl withdrawal in rats. *Neuropharmacology*, *55*(5), pp.812-818.
11. Alipio JB, Haga C, Fox ME, Arakawa K, Balaji R, Cramer N, *et al*. (2021): Perinatal fentanyl exposure leads to long-lasting impairments in somatosensory circuit function and behavior. *Journal of Neuroscience*, *41*(15), pp.3400-3417.
12. Goetz TG, Becker JB, Mazure CM (2021): Women, opioid use and addiction. *The FASEB Journal*, *35*(2), p.e21303.
13. Alipio JB, Brockett AT, Fox ME, Tennyson SS, deBettencourt CA, El-Metwally D, *et al*. (2021): Enduring consequences of perinatal fentanyl exposure in mice. *Addiction biology*, *26*(2), p.e12895.
14. Chandra R, Engeln M, Francis TC, Konkalmatt P, Patel D, Lobo MK (2017): A role for peroxisome proliferator-activated receptor gamma coactivator-1α in nucleus accumbens neuron subtypes in cocaine action. *Biological psychiatry*, *81*(7), pp.564-572.
15. Engeln M, Song Y, Chandra R, La A, Fox ME, Evans B, *et al*. (2021): Individual differences in stereotypy and neuron subtype translatome with TrkB deletion. *Molecular psychiatry*, *26*(6), pp.1846-1859.
16. Zhou Y, Zhou B, Pache L, Chang M, Khodabakhshi AH, Tanaseichuk O, *et al*. (2019): Metascape provides a biologist-oriented resource for the analysis of systems-level datasets. *Nature communications*, *10*(1), pp.1-10.
17. Janky RS, Verfaillie A, Imrichová H, Van de Sande B, Standaert L, Christiaens V, *et al*. (2014): iRegulon: from a gene list to a gene regulatory network using large motif and track collections. *PLoS computational biology*, *10*(7), p.e1003731.
18. Visse R, Nagase H (2003): Matrix metalloproteinases and tissue inhibitors of metalloproteinases: structure, function, and biochemistry. *Circulation research*, *92*(8), pp.827-839.

19. Ray MH, Williams BR, Kuppe MK, Bryant CD, Logan RW (2022): A Glitch in the Matrix: The Role of Extracellular Matrix Remodeling in Opioid Use Disorder. *Frontiers in Integrative Neuroscience*, p.61.
20. Malinowska M, Tokarz-Deptuła B, Deptuła W (2017): Butyrophilins: an important new element of resistance. *Central European Journal of Immunology*, *42*(4), pp.399-403.
21. Tonks NK, Neel BG (2001): Combinatorial control of the specificity of protein tyrosine phosphatases. *Current opinion in cell biology*, *13*(2), pp.182-195.
22. Brady-Kalnay SM, Mourton T, Nixon JP, Pietz GE, Kinch M, Chen H, *et al*. (1998): Dynamic interaction of PTPμ with multiple cadherins in vivo. *The Journal of cell biology*, *141*(1), pp.287-296.
23. McCole DF (2013): Phosphatase regulation of intercellular junctions. *Tissue barriers*, *1*(5), p.e26713.
24. Browne CJ, Godino A, Salery M, Nestler EJ (2020): Epigenetic mechanisms of opioid addiction. *Biological psychiatry*, *87*(1), pp.22-33.
25. Calarco CA, Fox ME, Van Terheyden S, Turner MD, Alipio JB, Chandra R, *et al*. (2021): Mitochondria-related nuclear gene expression in the nucleus accumbens and blood mitochondrial copy number after developmental fentanyl exposure in adolescent male and female C57BL/6 mice. *Frontiers in psychiatry*, p.1910.
26. Mendez EF, Wei H, Hu R, Stertz L, Fries GR, Wu X, *et al*. (2021): Angiogenic gene networks are dysregulated in opioid use disorder: evidence from multi-omics and imaging of postmortem human brain. *Molecular psychiatry*, *26*(12), pp.7803-7812.
27. Feng Y (2008): Convergence and divergence in the etiology of myelin impairment in psychiatric disorders and drug addiction. *Neurochemical research*, *33*(10), pp.1940-1949.
28. Kumar M, Rainville JR, Williams K, Lile JA, Hodes GE, Vassoler FM, *et al*. (2021): Sexually dimorphic neuroimmune response to chronic opioid treatment and withdrawal. *Neuropharmacology*, *186*, p.108469.
29. Conte I, Morcillo J, Bovolenta P (2005): Comparative analysis of Six3 and Six6 distribution in the developing and adult mouse brain. *Developmental dynamics, Nov; 234(3):718-25*.
30. Wegner M, Riethmacher D (2001): Chronicles of a switch hunt: gcm genes in development. *Trends in Genetics. May 1;17(5):286-90*.
31. Simon NW, Moghaddam B (2015): Neural processing of reward in adolescent rodents. *Developmental Cognitive Neuroscience, Feb; 11:145-154*.
32. Doherty JM, Cooke BM, Frantz KJ (2013): A role for the prefrontal cortex in heroin-seeking after forced abstinence by adult male rats but not adolescents. *Neuropsychopharmacology, Feb; 38(3): 446-54*.
33. Fujihara Y, Noda T, Kobayashi K, Oji A, Kobayashi S, Matsumura T, *et al*. (2019): Identification of multiple male reproductive tract-specific proteins that regulate sperm migration through the oviduct in mice. *Proceedings of the National Academy of Sciences, Sep 10; 116(37): 18498-506*.
34. Bucan M, Abrahams BS, Wang K, Glessner JT, Herman EI, Sonnenblick LI, *et al*. (2009): Genome-wide analyses of exonic copy number variants in a family-based study point to novel autism susceptibility genes. *PLos genetics, Jun 26;5(6):e1000536*.
35. Ge G, Greenspan DS (2006): Developmental roles of the BMP/TLD metalloproteinases. *Birth Defects Research Part C: Embryo Today: Reviews Mar;78(1):47-68*.
36. Chandra R, Engeln M, Schiefer C, Patton MH, Martin JA, Werner CT, *et al*. (2017): Drp1 mitochondrial fission in D1 neurons mediates behavioral and cellular plasticity during early cocaine abstinence. *Neuron*, *96*(6), pp.1327-1341.
37. Wojcieszak J, Andrzejczak D, Szymańska B, Zawilska JB (2019): Induction of immediate early genes expression in the mouse striatum following acute administration of synthetic cathinones. *Pharmacological Reports. Dec 1;71(6):977-82*.
38. Chin MH, Qian WJ, Wang H, Petyuk VA, Bloom JS, Sforza DM, *et al*. (2008): Mitochondrial dysfunction, oxidative stress, and apoptosis revealed by proteomic and transcriptomic analyses of the striata in two mouse models of Parkinson's disease. *Journal of proteome research. Feb 1;7(2);666-77*.
39. Dityatev A, Schachner M, Sonderegger P (2010): The dual role of the extracellular matrix in synaptic plasticity and homeostasis. *Nature Reviews Neuroscience*, *11*(11), pp.735-746.

40. Ishiguro H, Liu QR, Gong JP, Hall FS, Ujike H, Morales M, *et al*. (2006): NrCAM in addiction vulnerability: positional cloning, drug-regulation, haplotype-specific expression, and altered drug reward in knockout mice. *Neuropsychopharmacology*, *31*(3), pp.572-584.
41. Ikeda H, Miyatake M, Koshikawa N, Ochiai K, Yamada K, Kiss A, *et al*. (2010): Morphine modulation of thrombospondin levels in astrocytes and its implications for neurite outgrowth and synapse formation. *Journal of biological chemistry*, *285*(49), pp.38415-38427.
42. Chioma VC, Kruyer A, Bobadilla AC, Angelis A, Ellison Z, Hodebourg R, *et al*. (2021): Heroin seeking and extinction from seeking activate matrix metalloproteinases at synapses on distinct subpopulations of accumbens cells. *Biological Psychiatry*, *89*(10), pp.947-958.
43. Kovatsi L, Batzios S, Nikolaou K, Fragou D, Njau S, Tsatsakis A, *et al*. (2013): Alterations in serum MMP and TIMP concentrations following chronic heroin abuse. *Toxicology mechanisms and methods*, *23*(5), pp.377-381.
44. Tapocik JD, Luu TV, Mayo CL, Wang BD, Doyle E, Lee AD, *et al*. (2013): Neuroplasticity, axonal guidance and micro-RNA genes are associated with morphine self-administration behavior. *Addiction biology May;18(3):480-95*.
45. Yuferov V, Zhang Y, Liang Y, Zhao C, Randesi M, Kreek MJ (2018): Oxycodone self-administration induces alterations in expression of integrin, semaphoring and ephrin genes in the mouse striatum. *Frontiers in Psychiatry Jun 12;9:257*.
46. Robinson TE, Kolb B (2004): Structural plasticity associated with exposure to drugs of abuse. *Neuropharmacology*, *47*, pp.33-46.
47. Diana M, Spiga S, Acquas E (2006): Persistent and reversible morphine withdrawal-induced morphological changes in the nucleus accumbens. *Annals of the New York Academy of Sciences*, *1074*(1), pp.446-457.
48. Graziane NM, Sun S, Wright WJ, Jang D, Liu Z, Huang YH, *et al*. (2016): Opposing mechanisms mediate morphine-and cocaine-induced generation of silent synapses. *Nature neuroscience*, *19*(7), pp.915-925.
49. Fox ME, Wulff AB, Franco D, Choi EY, Calarco CA, Engeln M, *et al*. (2022): Adaptations in nucleus accumbens neuron subtypes mediate negative affective behaviors in fentanyl abstinence, *Biological Psychiatry, (In press)*, doi: https://doi.org/10.1016/j.biopsych.2022.08.023.
50. Francis TC, Chandra R, Gaynor A, Konkalmatt P, Metzbower SR, Evans B, *et al*. (2017): Molecular basis of dendritic atrophy and activity in stress susceptibility. *Molecular psychiatry*, *22*(11), pp.1512-1519.
51. Francis TC, Gaynor A, Chandra R, Fox ME, Lobo MK (2019): The selective RhoA inhibitor rhosin promotes stress resiliency through enhancing D1-medium spiny neuron plasticity and reducing hyperexcitability. *Biological psychiatry*, *85*(12), pp.1001-1010.
52. Fox ME, Chandra R, Menken MS, Larkin EJ, Nam H, Engeln M, *et al*. (2020): Dendritic remodeling of D1 neurons by RhoA/Rho-kinase mediates depression-like behavior. *Molecular psychiatry*, *25*(5), pp.1022-1034.
53. Chartoff EH, McHugh RK (2016): Translational studies of sex differences in sensitivity to opioid addiction. *Neuropsychopharmacology Jan;41(1):383*.
54. Frost JL, Schafer DP (2016): Microglia: architects of the developing nervous system. Trends in cell biology. Aug 1;26(8): 587-97.
55. Jantzie LL, Maxwell JR, Newville JC, Yellowhair TR, Kitase Y, Madurai N, *et al*. (2020): prenatal opioid exposure: the next neonatal neuroinflammatory disease. *Brain, behavior, and immunity. Feb 1;84:45-58*.
56. Huning L, Kunkel GR (2021): The ubiquitous transcriptional protein ZNF143 activates a diversity of genes while assisting to organize chromatin structure. *Gene. Feb 15;769:145205*.
57. Lu W, Chen Z, Zhang H, Wang Y, Luo Y, Huang P (2012): ZNF143 transcription factor mediates cell survival through upregulation of the GPX1 activity in the mitochondrial respiratory dysfunction. *Cell death Dis Nov 15;3(11): e422*.
58. Mulligan MK, Ponomarev I, Hitzemann RJ, Belknap JK, Tabakoff B, Harris RA, *et al*. (2006): Toward understanding the genetics of alcohol drinking through transcriptome meta-analysis. *Proceedings of the National Academy of Sciences Apr;18103(16):6368-73*.
59. Candice C (2012): Gene expression under the influence: Transcriptional profiling of ethanol in the brain. *Current Psychopharmacology Vol1(4) 301-314*.

List of Tables

**Mitochondria Respiration**

| | | | | | | | | |
|---|---|---|---|---|---|---|---|---|
| | **NAc** | | **VTA** | | **VTA** | | **S1** | |
| | **Males** | | **Males** | | **Females** | | **Females** | |
| **Gene** | **FDR** | **LogFC** | **FDR** | **LogFC** | **FDR** | **LogFC** | **FDR** | **LogFC** |
| ***Ndufa1*** | 0.01 | 0.6 | 1.46E-05 | -1.0 | | | | |
| ***Ndufa12*** | 0.007 | 0.3 | | | | | | |
| ***Ndufs4*** | 0.002 | 0.32 | | | | | | |
| ***Ndufa5*** | 0.017 | 0.48 | 0.0009 | -0.6 | | | 0.01 | 0.54 |
| ***Ndufs5*** | 0.008 | 0.36 | | | | | 0.01 | 0.36 |
| ***Ndufa4*** | 0.015 | 0.33 | | | | | 0.01 | 0.38 |
| ***Ndufb10*** | 0.001 | 0.37 | | | | | 0.001 | 0.42 |
| ***Ndufa7*** | 0.014 | 0.34 | 6.52E-06 | -0.59 | 0.02 | -0.4 | 0.0008 | 0.52 |
| ***Ndufb1-ps*** | 0.013 | 0.63 | 0.0037 | -0.67 | | | 0.002 | 0.86 |
| ***Ndufa11*** | | | 0.0007 | -0.43 | 0.02 | -0.44 | 0.01 | 0.38 |
| ***Ndufa2*** | | | 0.0009 | -0.67 | | | 0.002 | 0.77 |
| ***Ndufs7*** | | | 6.84E-06 | -0.62 | 0.02 | -0.44 | | |
| ***Ndufs6*** | | | 0.0001 | -0.61 | | | 0.01 | 0.49 |
| ***Ndufv3*** | | | 1.63E-06 | -0.53 | | | 0.005 | 0.38 |
| ***Ndufb8*** | | | 1.44E-06 | -0.99 | | | | |
| ***Ndufb3*** | | | 0.0018 | -0.39 | | | 0.03 | 0.34 |
| ***Ndufb11*** | | | 0.0008 | -0.37 | | | 0.025 | 0.31 |
| ***Ndufb7*** | | | 3.95E-07 | -0.8 | 0.019 | -0.5 | | |
| ***Ndufa3*** | | | 0.0001 | -0.88 | | | 0.01 | 0.68 |
| ***Ndufa13*** | | | 5.71E-07 | -0.84 | | | 0.01 | 0.48 |
| ***Ndufc1*** | | | 6.6E-05 | -0.61 | 0.04 | -0.47 | 0.02 | 0.43 |
| ***Ndufaf8*** | | | 8.05E-05 | -0.91 | | | | |
| ***Ndufa12-ps*** | | | 0.00028 | -1.15 | | | 0.01 | 0.94 |
| ***Ndufaf4*** | | | 1.68E-05 | 0.54 | | | | |
| ***Ndufb4*** | | | | | | | 0.04 | 0.4 |
| ***Ndufs5-ps*** | | | | | | | 0.027 | 0.6 |
| ***Ndufa6*** | | | 0.0036 | -0.39 | | | 0.039 | 0.35 |
| | | | | | | | | |

**Table 1**. Expression profile mitochondrial complex 1 NADH:ubiquinone oxidoreductase subunits in PFE. Red values indicate upregulation while blue values indicate downregulation. Significance level was set at FDR < 0.05; LogFC, log fold change.

**ECM and Neuronal guidance**

| | | | | |
|---|---|---|---|---|
| | **NAc** | | **VTA** | |
| | **Males** | | **Males** | |
| **Gene** | **FDR** | **LogFC** | **FDR** | **LogFC** |
| ***Col5a2*** | 0.01 | -0.81 | | |
| ***Col4a1*** | 0.005 | -0.41 | 0.001 | -0.43 |
| ***Col4a2*** | 0.01 | -0.41 | 2.72E-05 | -0.67 |
| ***Col6a3*** | 0.029 | -0.84 | | |
| ***Col5a3*** | | | 0.001 | -0.85 |
| ***Col20a1*** | | | 0.005 | -0.68 |
| ***Col6a2*** | | | 0.01 | -0.86 |
| ***Col2a1*** | | | 0.01 | -0.8 |
| ***Col11a2*** | | | 2.03E-05 | -0.82 |
| ***Col7a1*** | | | 1.8E-05 | -1.2 |
| ***Col5a1*** | | | 0.01 | -0.89 |
| ***Col9a3*** | | | 0.001 | -0.98 |
| ***Col9a2*** | | | 0.004 | -0.79 |
| ***Col16a1*** | | | 0.001 | -0.61 |
| ***Fbn1*** | 0.0047 | -0.77 | | |
| ***Fbn2*** | 0.02 | -0.66 | | |
| ***Notch1*** | 0.005 | -0.46 | 0.01 | -0.36 |
| ***Notch2*** | 0.03 | -0.55 | | |
| ***Notch3*** | 0.04 | -0.37 | 0.0003 | -0.58 |
| ***Notch4*** | | | 0.0006 | -0.63 |
| ***Ntn1*** | 0.03 | -0.57 | 0.004 | -0.71 |
| ***Lama5*** | 0.004 | -0.55 | 1.15E-05 | -0.8 |
| ***Frem2*** | 0.04 | -0.55 | | |
| ***Ltbp4*** | 0.01 | -0.44 | 7.56E-05 | -0.69 |
| ***Gpc6*** | 0.03 | -0.48 | | |
| ***Tnr*** | 0.01 | -0.38 | | |
| ***Plxnb1*** | 0.00007 | -0.4 | 0.0008 | -0.36 |
| ***Plxnb2*** | 0.03 | -0.35 | 0.005 | -0.41 |
| ***Plxna1*** | 0.0002 | -0.69 | 0.02 | -0.38 |
| ***Plxna3*** | 0.01 | -0.47 | 0.03 | -0.37 |
| ***Nav1*** | 0.004 | -0.32 | | |
| ***Nav2*** | 0.01 | -0.37 | | |
| ***Slit1*** | 0.04 | -0.66 | | |
| ***Slit2*** | 0.009 | -0.9 | | |
| ***Efna5*** | 0.02 | -0.36 | | |

**Table 2.** Expression profile of ECM signaling molecules and neuronal guidance genes downregulated specifically in the NAc and VTA of male juvenile mice exposed to perinatal fentanyl. Significance level was set at FDR < 0.05.; LogFC, log fold change.

**Vesicular and synaptic signaling**

| | | | | |
|---|---|---|---|---|
| | **NAc** | | **VTA** | |
| | **Females** | | **Males** | |
| **Gene** | **FDR** | **LogFC** | **FDR** | **LogFC** |
| ***Adra2a*** | 0.03 | -1.03 | | |
| ***Dlgap1*** | 0.02 | -0.66 | | |
| ***Flot1*** | 0.04 | -0.44 | 0.02 | -0.36 |
| ***Elav14*** | 0.03 | -0.72 | | |
| ***Napb*** | 0.03 | -0.72 | | |
| ***Nrg3*** | 0.04 | -0.62 | | |
| ***Prkce*** | 0.03 | -0.34 | | |
| ***Slc30a3*** | 0.04 | -1.73 | | |
| ***Cadps*** | 0.04 | -0.47 | | |
| ***Cabp1*** | 0.03 | -0.69 | | |
| ***Olfm1*** | 0.03 | -0.92 | | |
| ***Nptxr*** | 0.04 | -1.04 | | |
| ***Ntng2*** | 0.04 | -0.91 | | |
| ***Neurod1*** | 0.03 | -1.59 | | |
| ***Abat*** | 0.02 | 0.38 | | |
| ***Unc13c*** | 0.02 | 0.87 | | |
| ***Lrrtm3*** | 0.04 | 0.45 | | |

**Table 3.** Expression profile of some vesicular and synaptic signaling genes specifically dysregulated in NAc of female juvenile mice exposed to perinatal fentanyl. Red values indicate upregulation while blue values indicate downregulation. Significance level was set at FDR < 0.05. LogFC, log fold change.

List of Figures

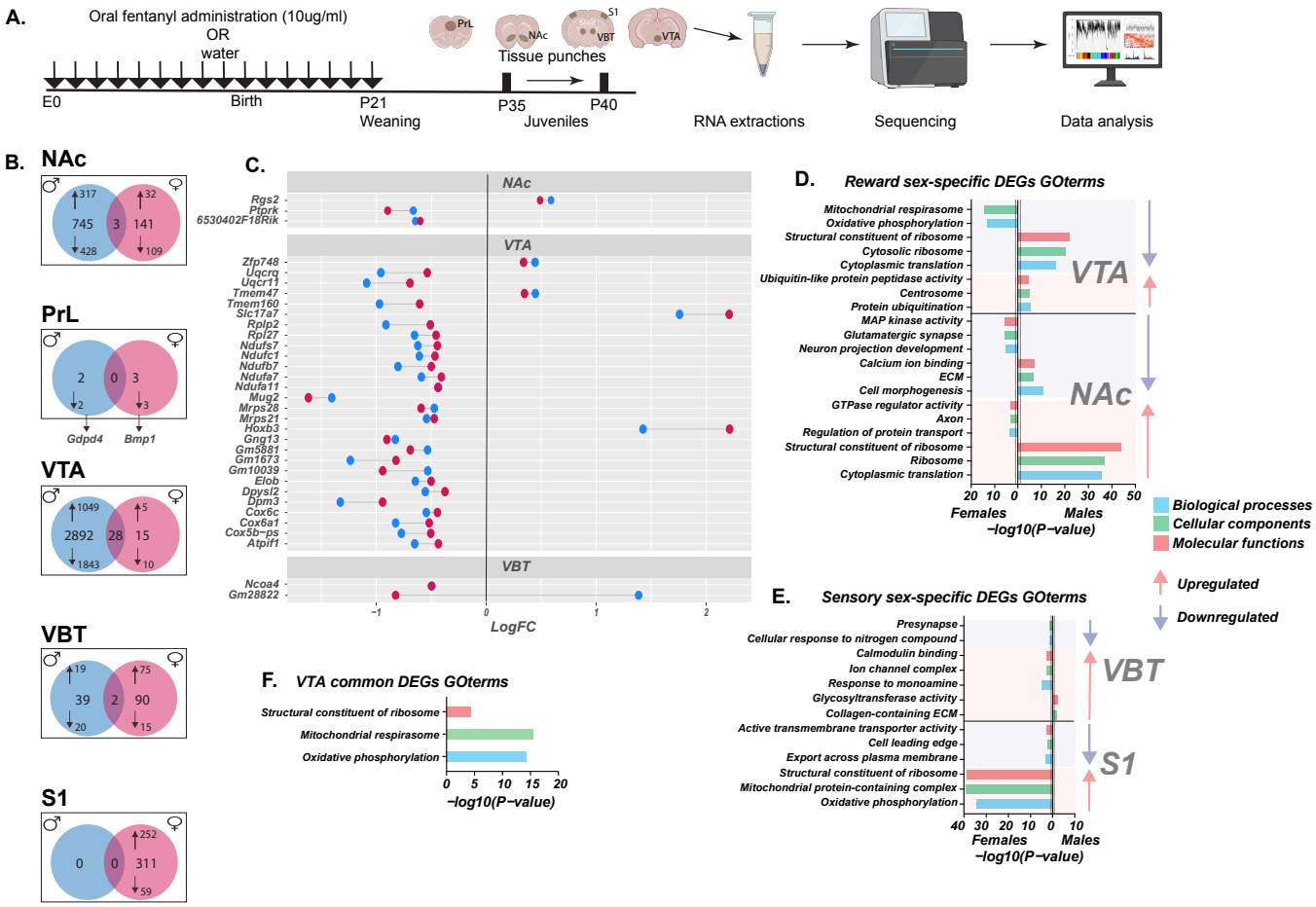


**Figure 1. Transcriptomic profiling of reward and sensory brain areas of PFE juvenile mice.** (A) Schematic of experimental design and pipeline. Pregnant C57/BL6 mice were administered 10µg/ml fentanyl in drinking water from E0 through birth till weaning of pups at P21. Between P35 and P40, 4 mice/treatment/sex were sacrificed, and tissue punches were collected from PrL with a single midline 12-gauge, NAc and VBT with bilateral 14-gauge, VTA with a single midline 14-gauge and S1 with bilateral 15-gauge. Thereafter, RNAs were extracted from tissue punches and sequenced. Following quality control, subsequent transcriptomic analyses was done with significance set at uncorrected p <0.05. (B) Venn diagram of DE transcripts across brain areas using an FDR of < 0.05 and Log Fold Change (LogFC) cut-off of +/- 0.3. (C) and (D) Gene Ontology Enrichment analyses on significantly altered sex-specific DEGs across reward (C) Expression profile of common DEGs between males (blue) and females (red) altered by PFE. (D) and (E) Gene Ontology Enrichment of sex-specific DEGs altered by PFE across reward (D) and sensory (E) areas. (F) Gene Ontology Enrichment of common VTA DEGs altered by PFE. Blue bars (BP), green bars (CC) and red bars (MF). Y-axis indicates top enrichment terms and X-axis indicates significance level of enrichment. Blue and red arrows indicate expression pattern of enriched terms by sex. PFE, perinatal fentanyl exposed; E0, embryonic day 0; P21, P35 and P40, postnatal days 21, 35 and 40; PrL, prelimbic cortex; NAc, nucleus accumbens; VBT, ventrobasal thalamus; VTA, ventral tegmental area; S1, somatosensory area 1; DE, differentially expressed; DEGs, differentially expressed genes, BP, biological processes; CC, cellular components; MF, molecular functions.

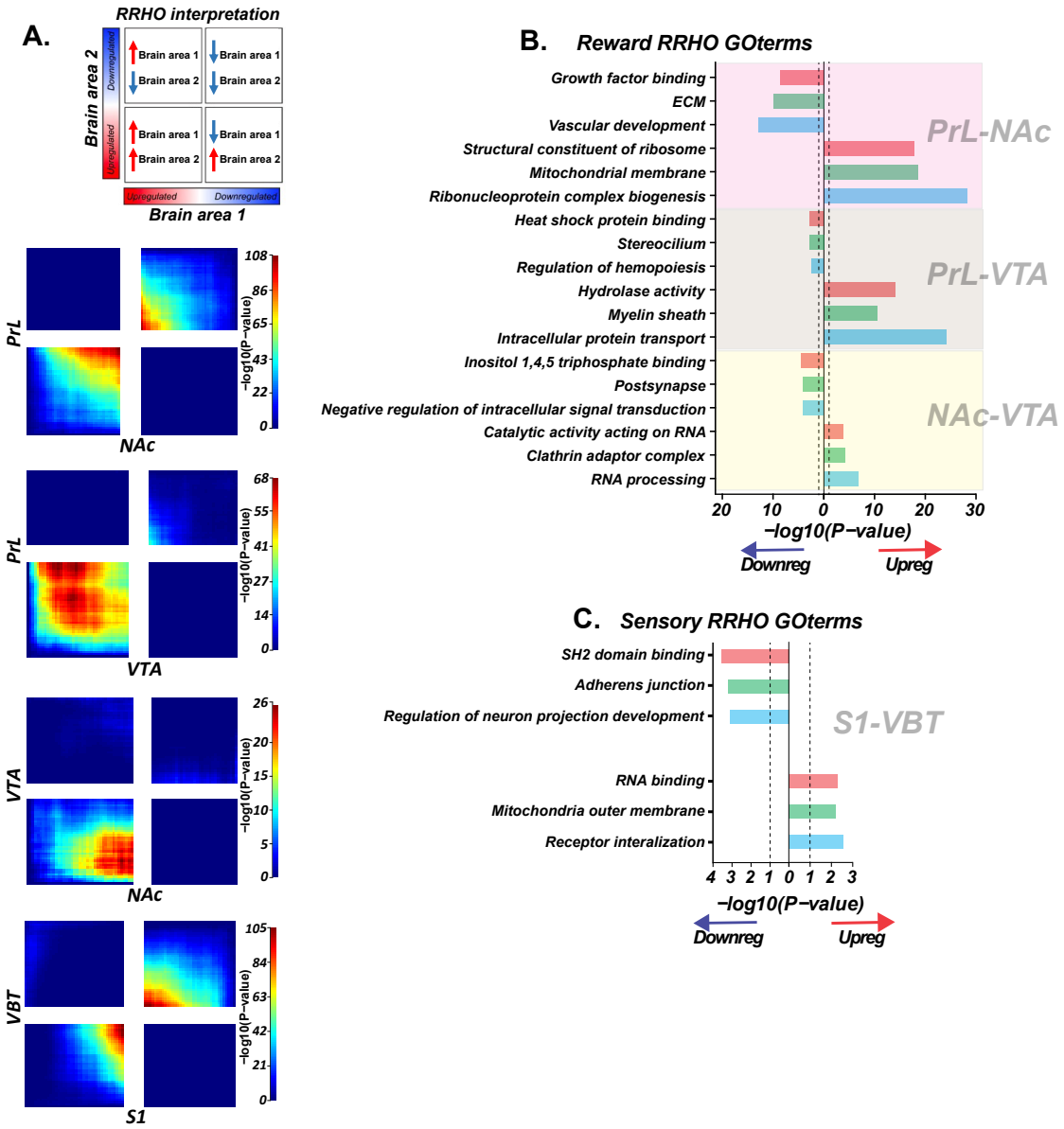


**Figure 2. High transcriptional concordance reveals commonly altered enrichment terms between brain regions associated with PFE mice.** (A) RRHO plot showing high degree of transcriptional concordance between PrL-NAc, PrL-VTA, VTA-NAc and VBT-S1 in PFE mice. (B) and (C) Enrichment analyses of threshold-free DE transcript overlap from RRHO across reward (B) and sensory (C) areas. Blue bars (BP), green bars (CC) and red bars (MF). Y-axis indicate top enrichment and X-axis indicate significance level of enrichment. Blue and red arrows indicate expression pattern of enriched terms by sex. PFE, perinatal fentanyl exposed; PrL, prelimbic cortex; NAc, nucleus accumbens; VBT, ventrobasal thalamus; VTA, ventral tegmental area; S1, somatosensory area 1; DE, differentially expressed; DEGs, differentially expressed genes, BP, biological processes; CC, cellular components; MF, molecular functions.

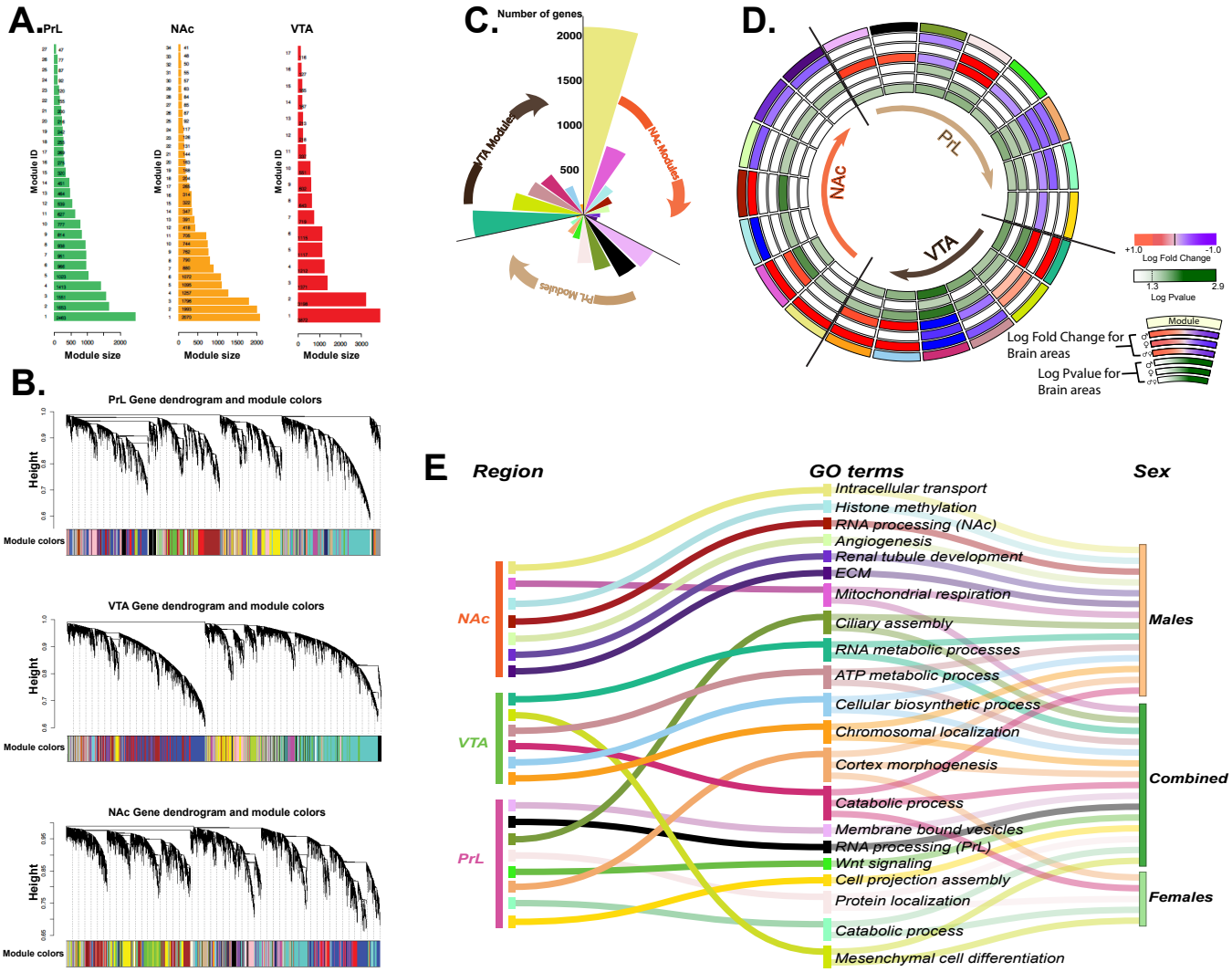


**Figure 3. Weighted gene co-expression network analyses (WGCNA) showing significant modules associated with fentanyl in a sex-specific manner in reward brain areas.** (A) Total number of reward module by sizes generated by WGCNA. Modules are ordered numerically by size. (B). Reward brain area dendrograms produced by hierarchical clustering on dissimilarity matrix derived from a topological overlap matrix representing both direct and indirect relationships between genes. (C) Circular bar plot showing significant modules associated with fentanyl. Each bar on plot is arbitrarily color coded to denote a module. The size of each bar represents the number of genes within the module. (D) Circos plot showing modules in a clockwise fashion from PrL, VTA and NAc. Each pie represents a module with outermost segment retaining module color, and inner 3 segments containing fold change in expression for male, female and common genes associated with fentanyl respectively, and innermost 3 segments representing -$\log_{10}$($P$ values) respectively. (E) Sankey plot showing description of top gene ontology enrichment for each significant module.

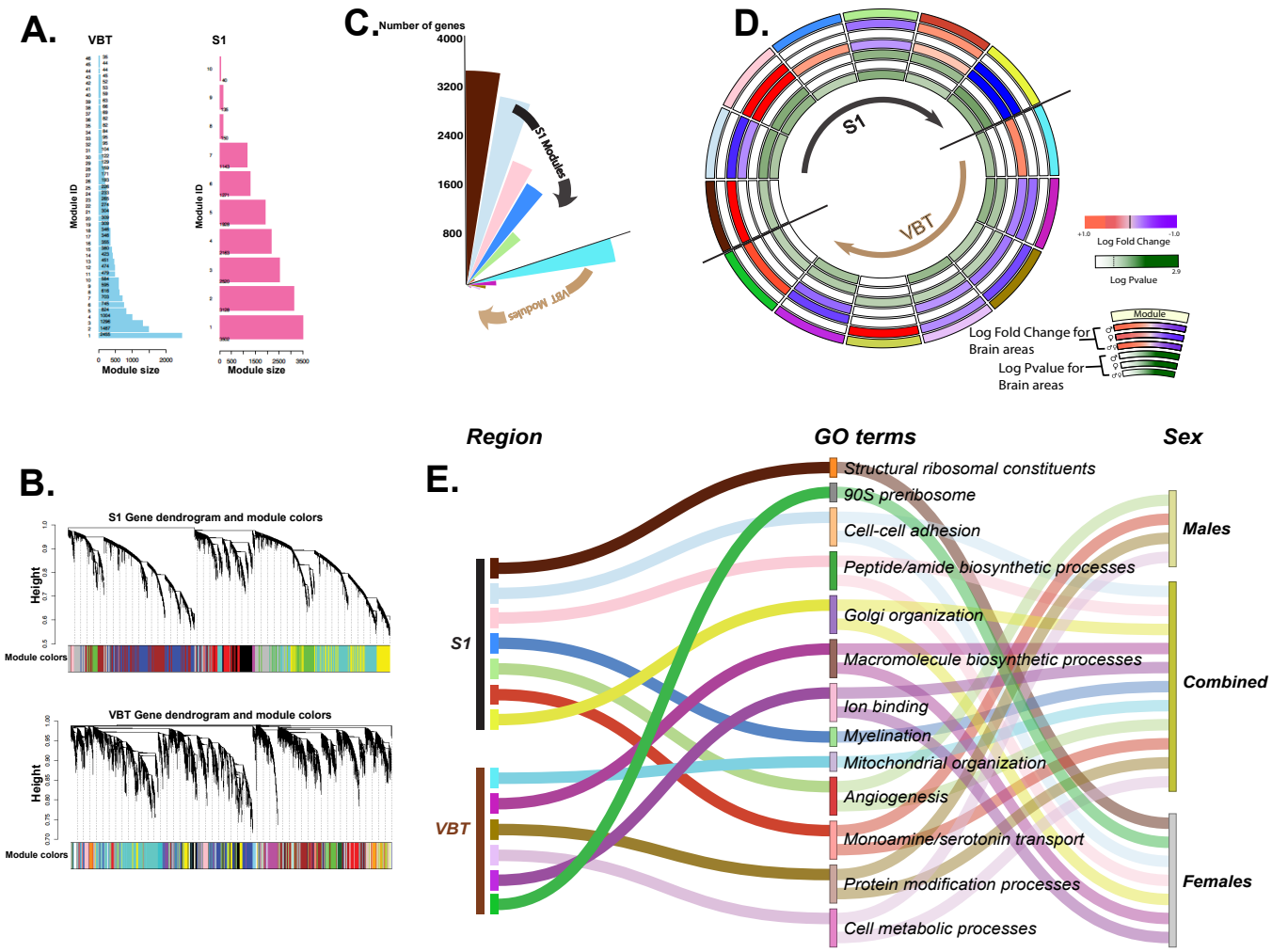


**Figure 4. WGCNA showing significant modules associated with fentanyl in a sex-specific manner in sensory brain areas.** (A) Total number of sensory module by sizes generated by WGCNA. Modules are ordered numerically by size. (B). Sensory brain area dendrograms produced by hierarchical clustering on dissimilarity matrix derived from a topological overlap matrix representing both direct and indirect relationships between genes. (C) Circular bar plot with significant modules associated with fentanyl. Each bar on plot is arbitrarily color coded to denote a significant module. The size of each bar represents the number of genes within the module. (D) Circos plot showing modules in a clockwise fashion from S1 to VBT. Each pie represents a module with outermost segment retaining module color and inner 3 segments containing fold change in expression for male, female and common genes associated with fentanyl respectively, and innermost 3 segments representing -$\log_{10}$($P$ values) respectively. (E) Sankey plot showing description of top gene ontology enrichment for each significant module.

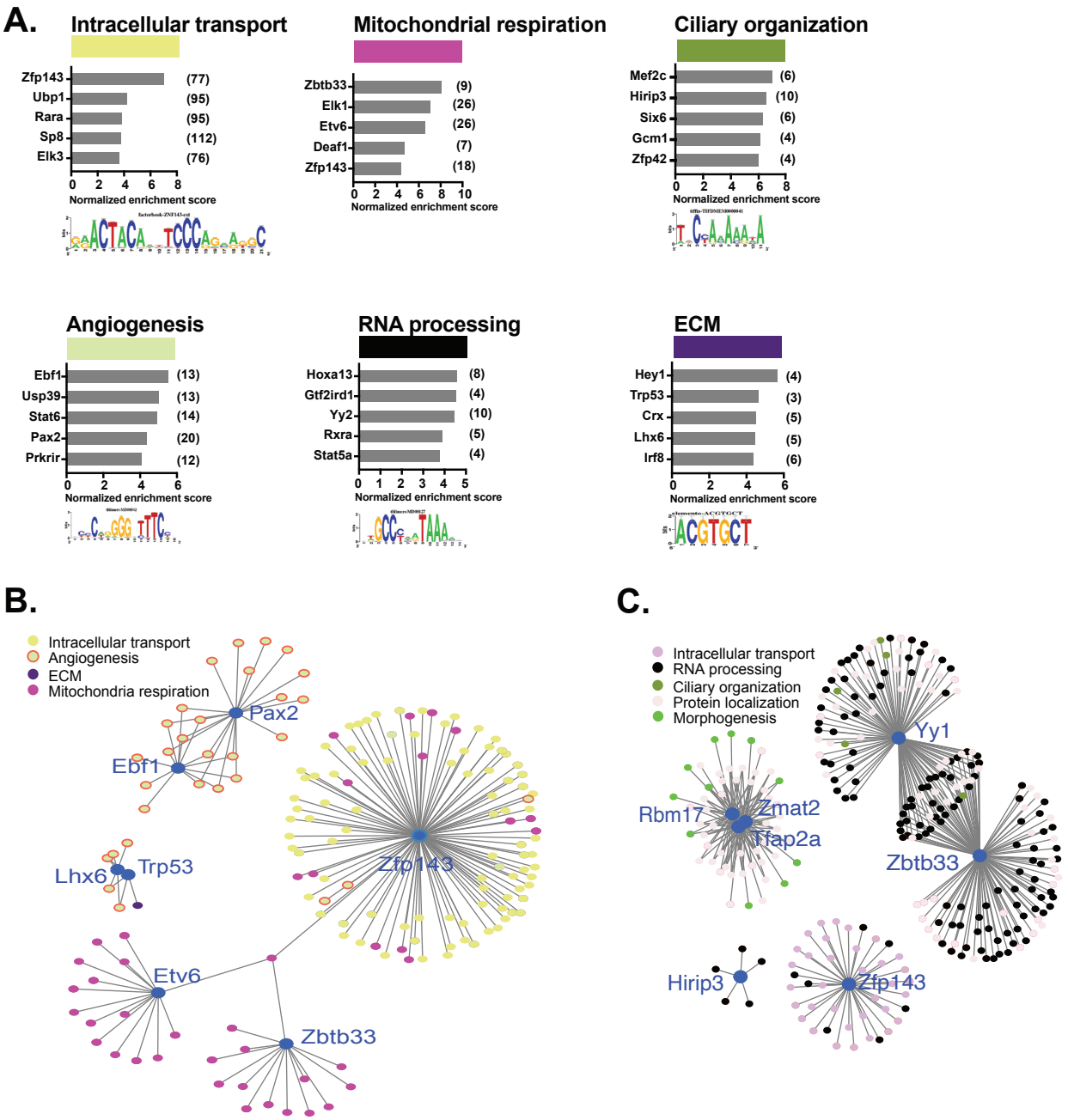


**Figure 5. Transcription factors (TFs) predicted with iRegulon for selected biological processes altered in reward and sensory brain areas of PFE mice.** (A). Bar graphs showing top 5 TFs predicted to regulate biological processes we observed to re-occur across all 5 brain areas. The biological processes represented here are 6 modules shown with their colors. X-axis shows normalized enrichment scores (NES). In brackets are number of downstream genes regulated by each TF. Below each graph are the predicted binding motifs of TF with highest NES. (B) and (C) Network showing highlighted TFs predicted to regulate selected processes across brain regions.